Contents lists available at ScienceDirect

Nuclear Instruments and Methods in Physics Research A

journal homepage: www.elsevier.com/locate/nima

A Study of the Non-uniformity of the PMT Photocathode Response and its Influence on the Results Obtained in Different Scintillation Experiments

V. Todorov [a], P. Cassette [a], Ch. Dutsov [b], B. Sabot [c], S. Georgiev [a], K. Mitev [a]

[a] Sofia University "St. Kliment Ohridski", Faculty of Physics, 5 James Bourchier Blvd, 1164 Bulgaria
[b] Paul Scherrer Institute, Villigen PSI, 5232, Switzerland
[c] Universite Paris-Saclay, CEA, LIST, Laboratoire National Henri Becquerel (LNE-LNHB), F-91120, France

a r t i c l e i n f o

Available ZZZZZ ZZZZ ZZZ

Keywords:
--
–
-- --

a b s t r a c t

This work presents an investigation on the non-uniformity of the response of the photocathode of two photomultiplier tubes (PMTs) and their potential influence on the results of scintillation measurements. An experimental system was developed which allows studies of the photocathode response non-uniformity and its influence on the shape of alpha spectra obtained after pulse-shape discrimination. The system is presented together with the tests of a Hamamatsu R7600U-200 and H11934-203 PMTs. A degradation of the counting efficiency and a shift of the peak position towards small values were identified in the measurements near the edges of the photocathode where the energy resolution is significantly worse compared to the central region of the PMT. Such non-uniformity also affects absolute activity measurements based on the free parameter model, i.e., the Triple to Double coincidence Ratio (TDCR) and the CIEMAT/NIST efficiency tracing methods. A significant non-uniformity of the response of a PMT would interfere with the assumption of the traditional free parameter model of a Poisson distribution of the number of emitted photons. This introduces an extra variance of the calculated detection efficiency which should be considered in the measurement uncertainty budget. Experimental results are presented in the paper, together with a discussion on their practical influence in scintillation measurements and absolute activity measurements.

1. Introduction

The non-uniformity of the response of photomultiplier tubes (PMT) has been studied in the past [1-2] and has been identified as one of the factors that can deteriorate the energy resolution in scintillation spectrometry [3-5]. In [6], after direct measurement, the position-dependent quantum efficiency of the photocathode is implemented in a Monte Carlo light transport code to study the energy resolution in a scintillation measurements and an increase of 11% in the energy resolution is observed. In a recent study [7] we have shown that, when analyzing alpha spectra obtained after pulse-shape discrimination (PSD) in measurements with plastic scintillators, the shape of the alpha peaks is distorted if there is a significant non-uniformity of the PMT response.

In general, more studies of the non-uniformity of the photocathode response are directed towards PMTs with large area photocathodes [8-10] with some indicating a relative change in photocathode efficiency as much as 40 – 50% [11].

The objective of this work was to develop an experimental system allowing the quantification of the non-uniformity of the photocathode response of the PMTs and to study the influence of this non-uniformity in various scintillation measurements like: the analysis of alpha spectra obtained after pulse-shape discrimination and the absolute activity measurements using the free parameter model in Liquid Scintillation Counting [12].

2. Methods and Materials

In this paper, the response of the photocathode of two PMTs – Hamamatsu R7600U-200 and Hamamatsu H11934-203 is studied. Both PMTs have a metal channel dynode structure with the R7600U-200 PMT having ten stages while the H11934 has 12 stages. Both PMTs have identical glass window size but significantly different effective area of the photocathode (see Fig. 1).

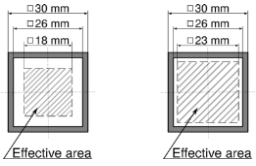

Figure 1. Size of the outer casing, the photocathode and the effective area of the R7600U-200 (left) and H11934-200 (right) PMT

In previous works, a serious non-uniformity of the photocathode response was identified in the Hamamatsu R7600-00-M4 PMTs [13] which have similar characteristics to R7600U-200. To the best of our knowledge, there are no published results for the photocathode response of the Hamamatsu H11934-203.

In order to study the non-uniformity of photocathode response of the Hamamatsu H11934-203 and R7600U-200 PMTs, two experimental systems were built. The first system, shown schematically in Fig. 2, consists of a homemade LED pulser (see Fig. 3), printed gray filters for adjusting the light intensity, a holder

Corresponding author. Tel.: +nn nn nn nn nn; fax: +ff ff f ff ff ff ff ff.
E-mail address: toto.titi@xxx.ff (A.FirstAuthor)

Doi :----------

for neutral density (ND) filters with certified transmission (Thorlabs NDK01), a fiber collimator followed by a multimode optical fiber with a 200 μm core diameter.

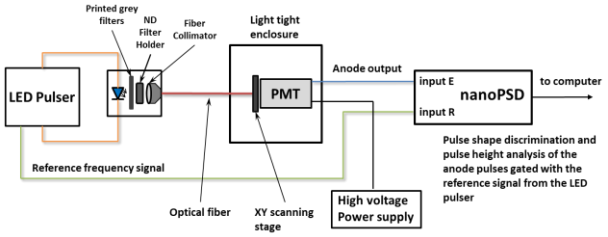

Figure 2. Experimental set-up to study the non-uniformity of the PMTs photocathode response

During the scans, the printed filters are fixed and no ND filters are placed in the holder. The fiber collimator collimates the light from the LED on one end of the optical fiber. The other end is touching the PMT window. The minimum step of the scanning stage is 0.1 mm in each direction which is achieved with a micrometer screw.

Using the coincidence counting functionality of the nanoPSD device [14], the anode signal of the PMTs is analyzed in coincidence with the reference frequency signal produced by the LED pulser. The ND filters are used for studying the linearity of PMT response by varying the intensity of the light incident on the photocathode. The acquisition time for each point in all scans for the study of the non-uniformity is 30 seconds.

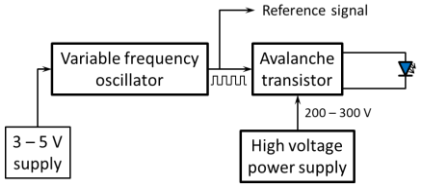

Figure 3. A scheme of the homemade LED pulser used in the experimental set-up. An LED (405 nm wavelength) is powered by a fast switching signal which frequency is governed by the variable frequency oscillator. The transistor works in avalanche mode and the time constant of the switch is about 0.25 ns.

The second developed system is shown in Fig. 4 show photos of a system for measuring the alpha spectra from the PSF200A plastic scintillator with ^{222}Rn absorbed in it. It consists of a 3D printed holder for the PMT and a 4×4 grid which is firmly fixed on top of the PMT window. The distance between the outermost edges of the grid is 26 mm. This ensures that the PS would be positioned within the glass window of the PMT. In order to reduce the photon loss, the PS piece (3×3×5 mm^3) is enveloped in reflective foil (3M Enhanced Specular Reflector) and fixed in a 3D printed plastic holder (5×5 mm^2). Between the scintillator and the reflective foil, a thin layer of silicon optical grease is applied. Optical grease is also deposited between the scintillator and the PMT window. The PSF200A scintillator has excellent α/β pulse-shape discrimination capabilities [15], which enabled us to study the changes in the alpha spectra of ^{222}Rn and its decay products when placing the scintillator on different positions on the grid.

Figure 4. Left: the grid fixed on the holder of the H11934 PMT; Center: the plastic scintillator piece inserted in a holder covered with reflective foil; Right: the PS holder slides through each hole in the grid ensuring that the PS touches the PMT window

The radioactive noble gas ^{222}Rn has advantageous properties for studying both the PSD capabilities and energy resolution of plastic scintillators. Radon can diffuse in the PS matrix. There it undergoes alpha decay ($E_{\alpha,Rn\text{-}222}$=5.489 MeV) with a half-life of 3.823(5) days. ^{222}Rn has four short-lived decay products: two beta emitters (^{214}Bi and ^{214}Pb) and two alpha emitters – ^{218}Po ($E_{\alpha,Po\text{-}218}$=6.002 MeV) and ^{214}Po ($E_{\alpha,Po\text{-}214}$=7.686 MeV). The emitted alpha particles have a short range. Thus, most of the α particles dissipate all their energy in the scintillator. However, due to the non-uniformity of the response of the photocathode, variations in both the PSD and pulse-height spectrum of the alpha particles is expected.

The signal processing is again accomplished with the nanoPSD analyzer which provides both pulse-height and pulse-shape discrimination. Thus, four spectra are obtained simultaneously: one PSD (Time-Invariant Pulse-shape Signature – TIPS) spectrum, and three pulse-height spectra: the raw pulse-height spectrum (α+β) and the separated alpha and beta spectra. An example of the real-time acquisition spectra is given in Figure 5. More details regarding the implementation of the method for pulse-shape discrimination can be found in [16].

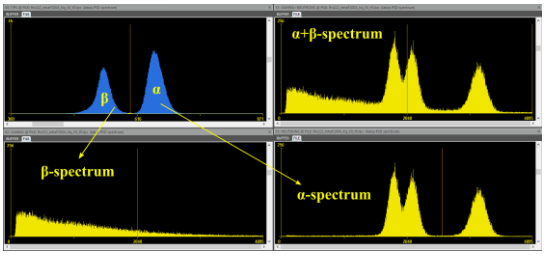

Figure 5. The nanoPSD program interface showing all four spectra. Top left: the PSD spectrum; top right: the raw pulse-height spectrum; bottom: the separated beta (left) and alpha (right) spectrum.

3. Results

3.1. Fine-step scanning of the photocathode

In this part of the study of the photocathode response, both H19934 and R7600U PMTs were scanned using the system presented in Fig. 2. Each PMT had a dedicated 3D printed holder which ensured that the PMT stayed fixed during the scans. In Fig. 6 a close-up photo of the PMT window is shown. A frame of reference used for the scan is also defined. Hereafter, the focusing electrodes of the PMTs, visible through the glass window, would be referred as ‘strips’.

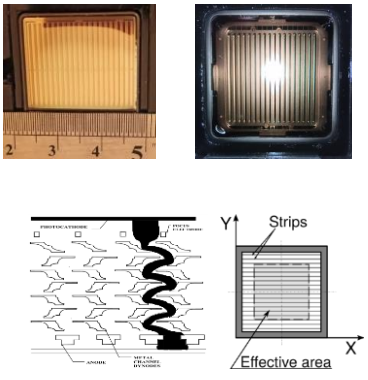

Figure 6. Top left: Photo of the H11934 PMT window; Top right: Photo of the R7600U PMT window; Bottom left: Transversal view of the metal channel dynode structure; Bottom right: A frame of reference used for the scans.

3.1.1. Scans of Hamamatsu H11934-203 PMT

Figure 7 shows the scans along the strips of the H11934 PMT. The high voltage supplied to the H11934 PMT during the scans is set to +1000 V. The slow and fast thresholds of the nanoPSD are both set to 30 to avoid noise pulses. The printed grey filters were used to decrease the intensity of the LED light. The

variation in the centroid position of the LED pulser peak is around 15% in the effective area of the photocathode (23×23 mm^2) but can be much greater in some scans. For example for Y=8 mm, the relative change between the maximum and minimum value is 33%. A definite peak in the central region along the strips of the PMT is due to a central wire in the middle of the PMT with a vertical orientation. (see Fig. 6 top left). It should be noted, however, that in another study [17] the area around the central wire of Hamamatsu H5783-06 PMT was found to decrease the photocathode response.

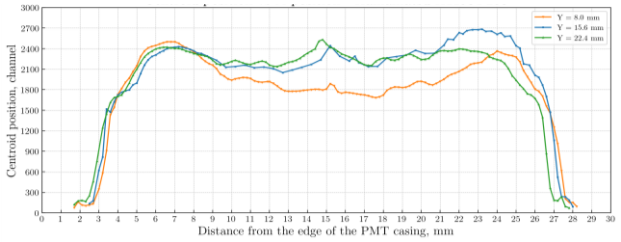

Figure 7. Plot of centroid position for scans along the strips of the photocathode for H11934 PMT.

Figure 8 shows the scans with the LED across the strips of Hamamatsu H11934 PMT.

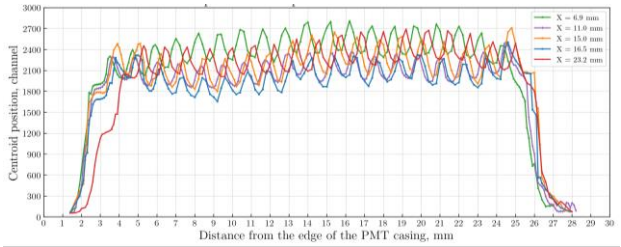

Figure 8. Plot of centroid position for scans across the strips of the photocathode for H11934 PMT.

Clearly, those scans reveal that the response of the photocathode significantly depends on where a photon is incident on the effective area of the photocathode. The observed periodic changes in the response can undoubtedly be attributed to the focusing electrodes of the PMT. However, the minimum and maximum values of the photocathode response are different along a single scan. This suggests that the photocathode response is also modulated by factors other than the multiplication structure of the PMT. It should be noted that the variation between the scans is substantial which might be expected by observing the great variation in the response along the strips (Fig. 7).

3.1.2. Scans of Hamamatsu R7600U-200 PMT

Figure 9 shows the scans with the R7600U PMT along the strips. For these scans, the high voltage supply is set to +850 V. The slow and fast thresholds of the nanoPSD are adjusted to 5 and 30, respectively.

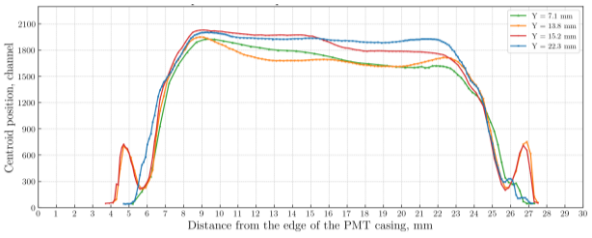

Figure 9. Plot of centroid position for scans along the strips of the photocathode for R7600U PMT.

The variation in the centroid position of the LED pulser peak is up to 17% in the effective area of the photocathode (18×18 mm^2). There are some noticeable peaks outside the effective area in the scans at Y=13.8 and 15.2 mm which could be caused by the metal attachments in the center of the first dynode (see Fig. 6, top right).

Scans across the strips of the R7600U PMT are presented in Figure 10. Similarly to the H11934 PMT, those scans quite well reveal the internal structure of the PMT and the response greatly varies between two peaks (or two valleys).

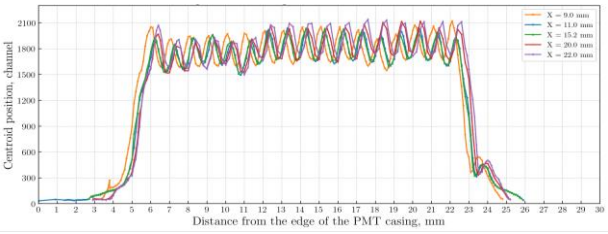

Figure 10. Plot of centroid position for scans across the strips of the photocathode for R7600U PMT.

There is a small peak at about 24 mm present in all scans and at X = 11, 15.2, 20.0 and 22.0 mm a drop appears at 11 mm. However, by viewing the PMT window it is difficult to unambiguously define the cause of these changes.

3.1. PMT response linearity measurements with respect to light intensity

To study the linearity of the PMT response we made measurements with optical filters with certified transmission (Thorlabs Neutral Density filters) which are placed after the printed grey filters (see Fig. 2). Figure 13 shows the LED spectra obtained after attenuating the light with filters of different optical transmission.

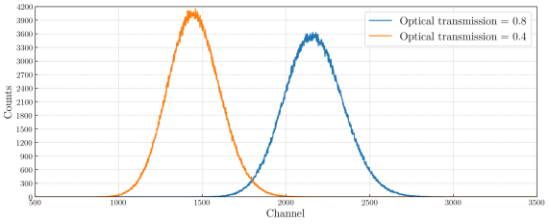

Figure 13. The LED spectrum after different attenuation of the light with ND filters. The optical transmission of the filters is 0.8 (blue line) and 0.4 (orange line).

3.2.1. Hamamatsu H11934-203 PMT

Figure 14 presents measurements with 7 different filters at one position on the effective area of the H11934 PMT with the supply voltage set to +1000 V.

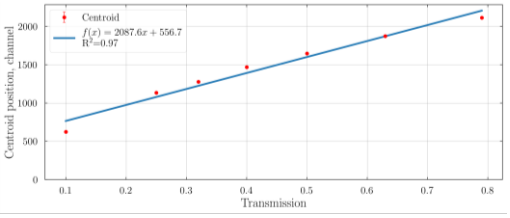

Figure 14. Plot of peak centroid position vs. light intensity incident on the H11934 PMT at +1000 V. The spectrum range is 4096 channels.

With the high voltage set to the maximum rate for this PMT, a non-linearity in the response of the PMT is observed. This could be attributed to saturation of the PMT divider response. Therefore the output current ceases to be proportional to the intensity of the incident light. The effect is known and discussed in [19].

However, when the supply voltage is decreased to +750 V,

which leads to lower anode current, the response of the PMT becomes linear (see Fig 15).

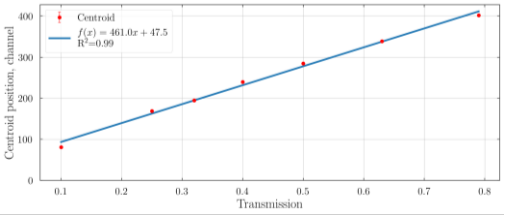

Figure 15. Plot of peak centroid position vs. light intensity incident on the H11934 PMT at +750 V. The spectrum range is 512 channels.

A significant spread of the experimental points is observed for measurements at random positions on the effective area of the photocathode (Fig 16). The contribution of the photocathode non-uniformity results in big dispersion between measurements even with the same optical filter. Moreover, the deviation would be more pronounced if measurements outside the effective area of the PMT are also included (not shown here).

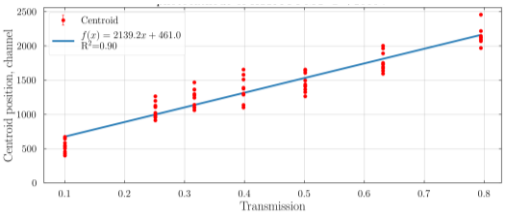

Figure 16. Plot of peak centroid position vs. light intensity incident on the H11934 PMT at +1000 V. The points corresponding to one optical transmission are measured on different random positions of the effective area of the photocathode. The spectrum range is 4096 channels.

3.2.2. Hamamatsu R7600U-200 PMT

Figure 15 presents the results from the linearity study of the R7600U PM. Similarly to the H11934 PMT, non-linearity in the response can be observed when measuring with high voltage allowing single-photon sensitivity.

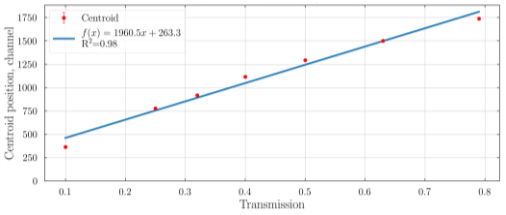

Figure 17. Plot of peak centroid position vs. light intensity incident on the R7600U PMT at +850 V. The spectrum range is 4096 channels.

Similarly to the H11934 PMT, linearity of the PMT response is achieved by decreasing the high voltage supplied to the PMT, avoiding saturation in the divider response. The results are presented in Fig 18, where excellent linearity is observed

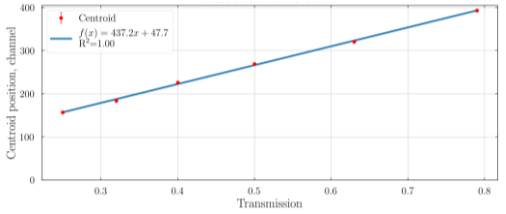

Figure 18. Plot of peak centroid position vs. light intensity incident on the R7600U PMT at +720 V. The spectrum range is 512 channels.

However, the non-uniformity of the photocathode response again introduces significant spread of the experimental point. This is shown in Fig. 19 where measurements on random points on the photocathode result in notable variation in the response for one filter.

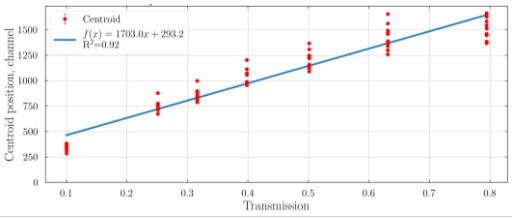

Figure 19. Plot of peak centroid position vs. light intensity incident on the R7600U PMT at +850 V. The points corresponding to one optical transmission are measured on different random positions of the effective area of the photocathode. The spectrum range is 4096 channels.

3.3. Influence of non-uniformity of the photocathode response on alpha-spectrometry

The PSF200A plastic scintillator with ^{222}Rn absorbed in it was used for the aim of this investigation. Two separate exposures to air with high (~100 MBq/m3) ^{222}Rn concentration of the same PS piece were made for the measurements with the H11934 and R7600U PMTs. The settings of the nanoPSD are set to automatic thresholds and the software range of the alpha-spectrum was set to 512 channels. For both PMTs the focusing electrodes are parallel to the columns of the grid and the frame of reference (Fig. 6 bottom right) is rotated 90° counter-clockwise. In the figures hereafter, 'X' denotes the columns of the grid and 'Y' denotes the rows.

The alpha-spectrum of ^{222}Rn and its decay products is obtained after pulse-shape discrimination. The nanoPSD analyzer provides four spectra: TIPS spectrum, the raw alpha and beta spectrum and the separated alpha and beta spectra. The pulse-shape discrimination is based on ballistic deficit measurement and digital time-invariant pulse shaping. The PMT signal is passed through slow and fast shapers. Then the pulse-height of each shape is measured using peak detectors. The TIPS is defined as the ratio of the maximum of the slow shaper and the maximum of the fast shaper [16]. The result for a PS in the center of the PMT window is well separated alpha and beta particles (see Fig. 5). This enables us to investigate the TIPS and alpha spectra and follow the changes in them when placing the PS on different points on the PMT photocathode.

3.3.1. Hamamatsu H11934-203 PMT

Figures 20 and 21 present the TIPS and the alpha spectra measured with the H11934 PMT. The high voltage supply was set to +750V. The spectra are acquired by consequently placing and measuring the PS spectrum in the openings of the grid (Fig. 4). The acquisition time is adjusted according to the counting rate and a predefined plan for the measurements.

Figure 20 shows the TIPS spectra obtained at different positions on the PMT photocathode. In order to evaluate the effect of the non-uniformity on the pulse-shape discrimination we use a figure of merit (FOM) defined as the difference between the maxima of two peaks divided by the sum of the FWHM of the peaks. The FOM is estimated by the algorithm available in the nanoPSD software.

From Fig. 20 it could be observed that the FOM of the spectra in the center of the grid is higher compared to the outer spectra which indicate that, indeed, the non-uniformity of the photocathode response has an influence on the pulse-shape discrimination. Although the FOM parameter is not affected by the non-uniformity as much as the energy resolution, it definitely repeats the variation in the energy resolution presented in Fig. 21.

From Fig. 21 it can be noted that in the center of the photocathode, the energy resolution is good enough that the ^{222}Rn and ^{218}Po α-peaks maxima are separated. This is not the case for the outer positions and especially in the corners where the quantum efficiency of the photocathode is low. There is also a notable difference between the spectra in the first and last columns with the former being with better energy resolution. Possible explanation for that is the higher quantum efficiency (high centroid position) in the

part of the PMT where Y>15 mm (see Fig. 8). The influence of the non-uniformity on the shape of α-peaks was studied in depth in [7] by measuring PS pieces of different sizes.

3.3.2. Hamamatsu R7600U-200 PMT

Figure 22 and 23 show the TIPS and the alpha spectra obtained with the Hamamatsu R7600U PMT. The grid position is the same as for the H11934 PMT but the high voltage supply is set to +720 V.

Figure 22 shows the TIPS spectra obtained at different positions of the PMT window. It can be seen that compared to the H11934 PMT there is a greater variance in the FOM value between the spectra. Furthermore, in the corners of the PMT window, the PSD is so degraded that the FOM cannot be estimated. This can be explained with the much smaller effective area.

Analogous to the measurements with the H11934 PMT, the maxima of ^{222}Rn and ^{218}Po peaks are separated only in the center of the PMT. Moreover, the peak of ^{214}Po alpha particles is also not separated in the outer spectra. This could be explained by the fact that except the four central positions, the PS piece is outside the effective area of the PMT. This, however, does not mask the variation in the energy resolution caused by the non-uniformity of the photocathode response and it can be observed between all spectra from the grid.

4. Discussion

The free parameter model is used in radionuclide metrology for the direct calibration of the activity of radionuclides [12]. In this model, the Poisson distribution of the number of photons emitted by the scintillation light pulse is traditionally used to calculate the detection efficiency from the non-detection efficiency, i.e., the probability that no photoelectron is detected. In case of a spatial non-uniformity of the PMT response, the mean value of the Poisson distribution, describing the intrinsic light yield of the detection process, is no more a constant value but becomes a random variable with a distribution taking into account the fluctuations of the detection process. This leads to a compound Poisson distribution. The non-detection efficiency calculation is similar to the one using a Poisson distribution, but its uncertainty is larger, due to the variability of the random variable describing the mean value of the compound Poisson distribution. This effect leads to an increase of the uncertainty of the detection efficiency, which becomes especially important in the measurement of low-energy radionuclides.

A possible solution would be to mask the most effective area of the PMTs which, in turn, equalizes the quantum efficiency of the photocathode. This idea has previously been explored in [20-22]. Although notable improvements in the resolution of the detection systems have been recorded, it comes with a caveat. That is, there is a non-negligible light loss which would make measurement of low-energy radionuclides practically impossible due to the low number of photons emitted. In addition, equipment capable of depositing precise amounts of masking material would be required due to the complex pattern of the non-uniformity of the studied PMTs. For now, the only reasonable solution in TDCR applications would be to mask the ineffective area of the R7600U PMT and to account for the larger detection uncertainty in the TDCR model.

5. Conclusion

In this work we have developed an experimental system to study the effects that the non-uniformity of the PMT response on the scintillation counting measurements. The effects of the non-uniformity of the PMT response have been described and quantified for scintillation detectors using Hamamatsu R7600U-200 and H11934-203 PMTs.

We identified a degradation of the counting efficiency and the energy resolution both in effective area and at the end of the PMTs. The large ineffective area of the R7600U-200 PMT causes significant problems in scintillation counting as it acts as a photon sink. The H11934 PMT has a smaller ineffective area but it still should be avoided (covered) in order to reduce the variance in scintillation counting experiments.

Experimentally, it has been shown that the non-uniformity of the PMT response has an adverse effect on the energy resolution of scintillation spectrometry and the pulse-shape discrimination. The effects of the non-uniformity of the PMT response regarding the radionuclide activity measurements using the free parameter model are discussed.

Acknowledgment

This work is supported by the Bulgarian National Scientific Research Fund under contract KP-06-H38/9 from 06.12.19 (TDCX).

References

[1]. Leskovar B, Lo CC, IEEE TNS 19(3) (1972) 50–62
[2].Godlove, T. F., & Wadey, W. G. (1954). Photocathode Uniformity and Resolution of Scintillation Spectrometers. In Review of Scientific Instruments (Vol. 25, Issue 1, pp. 1–4). AIP Publishing. https://doi.org/10.1063/1.1770874
[3]. Knoll GF (2010) Radiation Detection and Measurement. Wiley, New York
[4]. Schardt, A. W., & Bernstein, W. (1951). Resolution of the Scintillation Spectrometer. In Review of Scientific Instruments (Vol. 22, Issue 12, pp. 1020–1021). AIP Publishing. https://doi.org/10.1063/1.1745805
[5]. P. S. Takhar, "Resolution and Cathode Uniformity in Scintillation Counters," in IEEE Transactions on Nuclear Science, vol. 14, no. 1, pp. 438-442, Feb. 1967, doi: 10.1109/TNS.1967.4324451.
[6]. Mottaghian, M., Koohi-Fayegh, R., Ghal-Eh, N., & Etaati, G. R. (2010). Photocathode non-uniformity contribution to the energy resolution of scintillators. In Radiation Protection Dosimetry (Vol. 140, Issue 1, pp. 16–24). Oxford University Press (OUP). https://doi.org/10.1093/rpd/ncq041
[7]. Todorov, V. T., Dutsov, C. Ch., Cassette, P., & Mitev, K. K. (2022). Effects of the photocathode non-uniformity on radon measurements by plastic scintillation spectrometry. In Journal of Radioanalytical and Nuclear Chemistry. Springer Science and Business Media LLC. https://doi.org/10.1007/s10967-022-08362-6
[8]. Gao, F., Qian, S., Ma, Y., Xia, J., Ning, Z., Wang, Z., Ma, L., Wu, Q., & Peng, S. (2022). Research and development of 20-inch PMT uniformity scanning platform. In Nuclear Instruments and Methods in Physics Research Section A: Accelerators, Spectrometers, Detectors and Associated Equipment (Vol. 1027, p. 166257). Elsevier BV. https://doi.org/10.1016/j.nima.2021.166257
[9]. Kume, H., Sawaki, S., Ito, M., Arisaka, K., Kajita, T., Nishimura, A., & Suzuki, A. (1983). 20 inch diameter photomultiplier. In Nuclear Instruments and Methods in Physics Research (Vol. 205, Issue 3, pp. 443–449). Elsevier BV. https://doi.org/10.1016/0167-5087(83)90007-8
[10]. Unland Elorrieta, M. A., Busse, R. S., Classen, L., & Kappes, A. (2021). Homogeneity of the photocathode in the Hamamatsu R15458-02 Photomultiplier Tube. In Journal of Instrumentation (Vol. 16, Issue 11, p. P11038). IOP Publishing. https://doi.org/10.1088/1748-0221/16/11/p11038
[11]. Paul, J. M. (1970). Studies concerning the behaviour of photomultiplier with large photocathode. In Nuclear Instruments and Methods (Vol. 89, pp. 285–287). Elsevier BV. https://doi.org/10.1016/0029-554x(70)90836-0
[12]. Broda R. et al. Radionuclide metrology using liquid scintillation counting. Metrologia Vol 44 n° 4, 2007.
[13]. Kossakowski R, Audemer JC, Dubois JM, Fougeron D, Hermel R, et al. (2002) Study of the photomultiplier R7600-00-M4 for the purpose of the electromagnetic calorimeter in the AMS-02 experiment http://hal.in2p3.fr/in2p3-00021475
[14]. NanoPSD Yantel (labZY) https://www.yantel.com/products/nanopsd/
[15]. Mitev, K., Jordanov, V., Hamel, M., Dutsov, Ch., Georgiev, S., & Cassette, P. (2018). Development of a portable scintillation spectrometer with alpha-/beta- and neutron-/gamma- pulse-shape discrimination capabilities. In 2018 IEEE Nuclear Science Symposium and Medical Imaging Conference Proceedings (NSS/MIC). 2018 IEEE Nuclear Science Symposium and Medical Imaging Conference (NSS/MIC). IEEE. https://doi.org/10.1109/nssmic.2018.8824692
[16]. Jordanov VT, 2018 IEEE NSS MIC Conference Record https://doi.org/10.1109/nssmic.2018.8824502
[17]. Simeonov, V., Larcheveque, G., Quaglia, P., van den Bergh, H., & Calpini, B. (1999). Influence of the photomultiplier tube spatial uniformity on lidar signals. In Applied Optics (Vol. 38, Issue 24, p. 5186). The Optical Society. https://doi.org/10.1364/ao.38.005186
[18]. Brenner, R., Chou, H. P., Strauss, M. G., & Winiecki, A. L. (1982). Cathode Uniformity of New Square Photomultiplier Tubes. In IEEE Transactions on Nuclear Science (Vol. 29, Issue 1, pp. 207–211). Institute of Electrical and Electronics Engineers (IEEE). https://doi.org/10.1109/tns.1982.4335828
[19]. Photomultiplier Tubes Basics and Applications, 4th Edition, Hamamatsu Photonics K.K., 2017. URL https://www.hamamatsu.com/resources/pdf/etd/PMT_handbook_v4E.pdf
[20]. Dean, A. J., Dipper, N. A., Lewis, R. A., Lu Zho Guo, & Perotti, F. (1985). A diffusive light collection system for hard X-ray astronomical scintillation detectors. In Nuclear Instruments and Methods in Physics Research Section A: Accelerators, Spectrometers, Detectors and Associated Equipment (Vol. 236, Issue 2, pp. 410–413). Elsevier BV. https://doi.org/10.1016/0168-9002(85)90185-8
[21]. Veloso, J. F. C. A., dos Santos, J. M. F., & Conde, C. A. N. (1995). Large-window gas proportional scintillation counter with photosensor compensation. In IEEE Transactions on Nuclear Science (Vol. 42, Issue 4, pp. 369–373). Institute of Electrical and Electronics Engineers (IEEE). https://doi.org/10.1109/23.467818
[22]. Mead, J. B., & Martin, J. P. (1965). Improvement of resolution in large area photomultipliers. In Nuclear Instruments and Methods (Vol. 36, pp. 13–22). Elsevier BV. https://doi.org/10.1016/0029-554x(65)90400-3

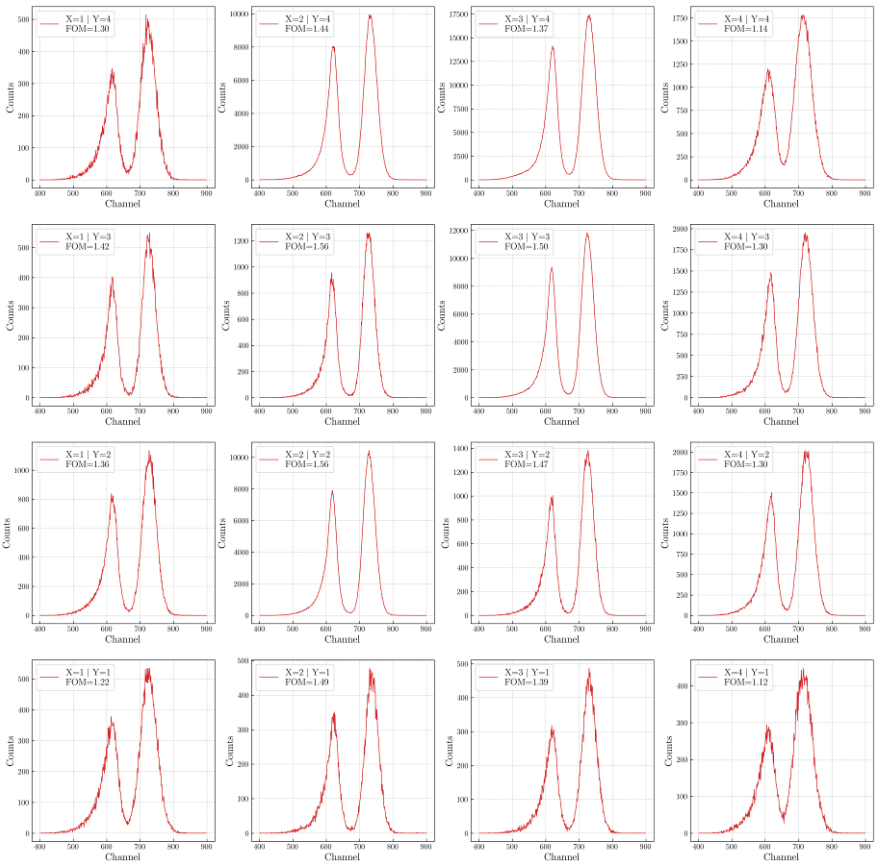

Figure 20. TIPS spectra of ^{222}Rn absorbed in PSF200A obtained at different positions on the photocathode of H11934-203 PMT. The estimated FOM of each spectrum is given in the legend.

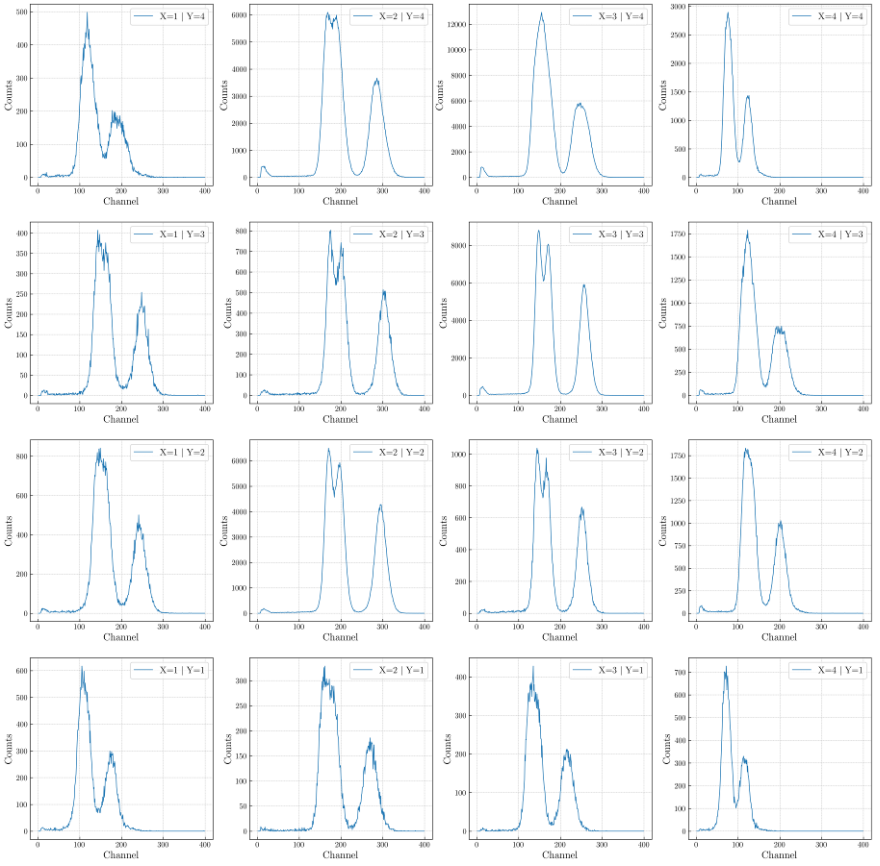

Figure 21. Pulse-height alpha spectra corresponding to the measurements shown in Figure 20.

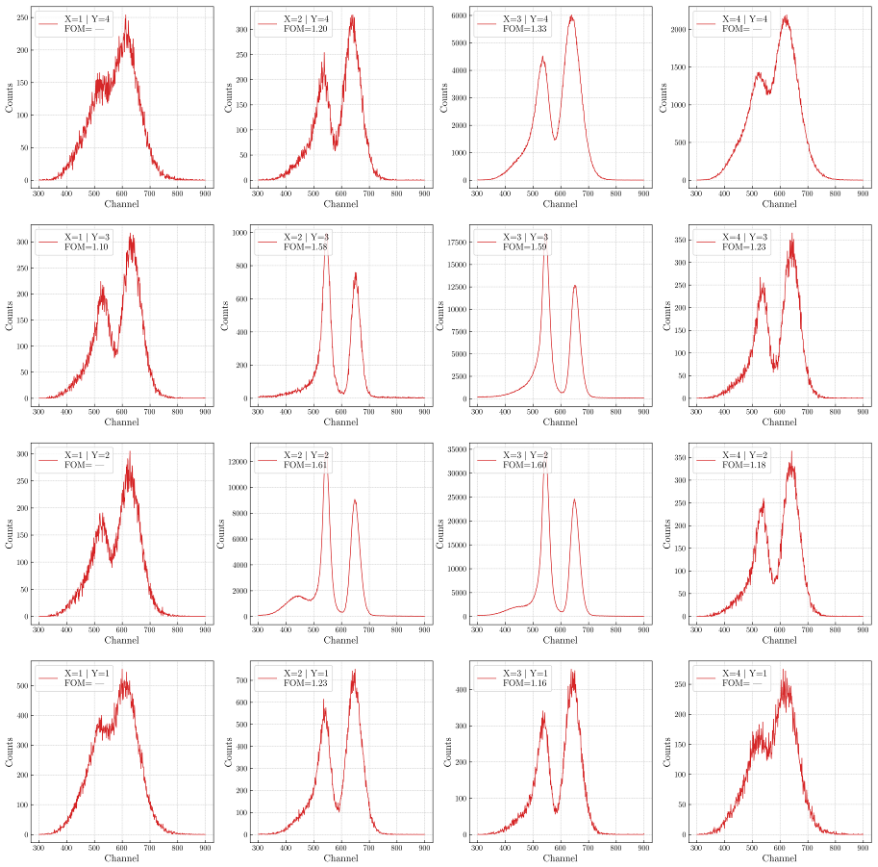

Figure 22. TIPS spectra of ^{222}Rn absorbed in PSF200A obtained at different positions on the photocathode of R7600U-200 PMT. The estimated FOM of each spectrum is given in the legend.

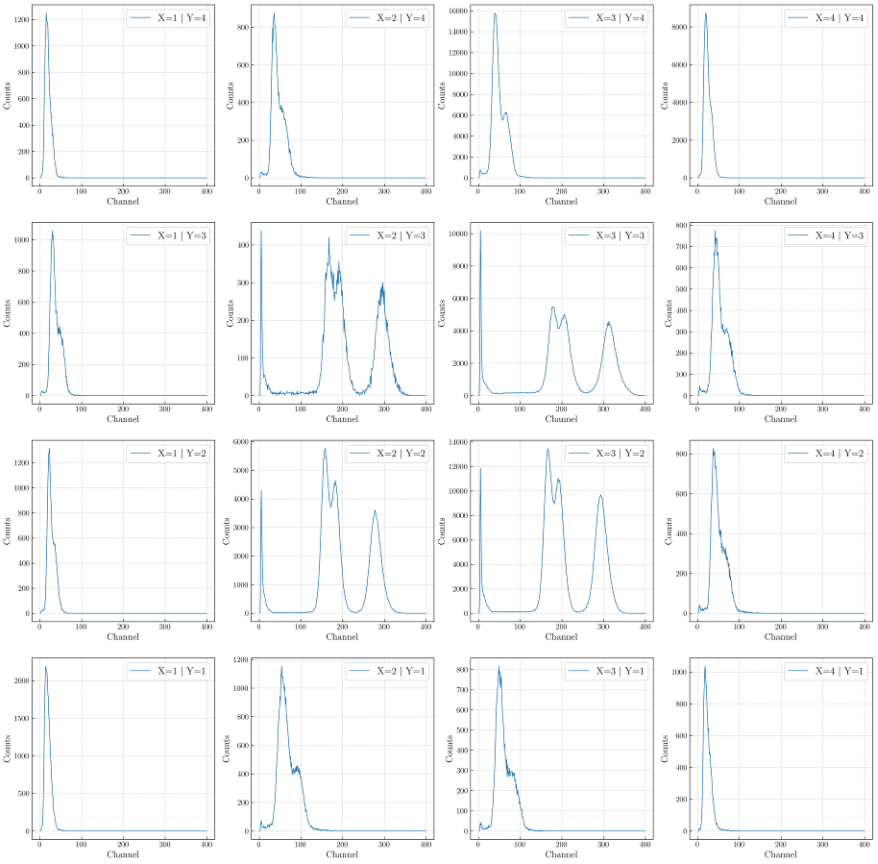

Figure 23. Pulse-height alpha spectra corresponding to the measurements shown in Figure 22.